

Evaluation of the Out-of-Plane Loads on a Submarine Undergoing a Steady Turn

Zhi Leong¹, Simon Piccolin², Marc Desjuzeur², Dev Ranmuthugala^{1,3} and Martin Renilson¹

¹Australian Maritime College, University of Tasmania, Launceston, Tasmania 7248, Australia

²ENSTA Bretagne, Brest 29806, France

³Defence Science and Technology Group, Fishermans Bend, Victoria 3207, Australia.

Abstract

When a submarine executes a turn in the horizontal plane, it experiences a pitching moment due to out-of-plane forces that push the stern downwards, giving an upward pitching moment. This study uses Computational Fluid Dynamics (CFD) to examine the distribution of the downward force over the stern.

Three different configurations of the generic Joubert submarine, which represents a contemporary conventional submarine, in a steady turn were examined. The three configurations were the: bare hull; hull and casing; and finally hull, casing and sail. The magnitude and location of the out-of-plane forces were obtained in each case.

Results show that both the sail and casing generate out-of-plane forces on the stern of the submarine when in a steady turn, although their effects on the submarine are different. The primary cause of the downward force over the stern is the presence of the sail. This is discussed in the paper with due regard to the hydrodynamic effects of the sail vortices on the flow around the submarine hull.

The developed CFD model will be used for further investigation of the out-of-plane forces and the phenomenon's dependence on the submarine turning angle, turning rate, and the shape and location of the submarine hull and sail. Understanding the phenomenon will contribute to further research and development into the hydrodynamics of submarines, both in the design and operational phases.

Nomenclature

B	Breadth (m)
L_{OA}	Overall length (m)
LC	Longitudinal location of the centre of origin from nose tip (m)
M	Pitching moment (N m)
M'	Non-dimensional pitching moment, $M/(0.5\rho U_0^2 L_{OA}^3)$
O	Centre of the submarine's local coordinate system
R	Turning radius (m)
T	Turning point (-)
u_*	Friction velocity ($m^2 s^{-1}$)
U_0	Linear velocity of the rotation at the vehicle's centre of origin ($m s^{-1}$)
r	Rotational velocity ($^\circ s^{-1}$)
r'	Non-dimensional rotational velocity, $r L_{OA}/U_0$
VC	Vertical location of the vehicle's centre of origin from its keel (m)
x, y, z	Cartesian coordinates in the x, y, z -direction (m)
y_{wall}	Distance of mesh node to the nearest wall surface (m)
y^+	Non-dimensional wall distance (-), $(u_* y_{wall})/\nu$
Z	Heave force, in the z -direction (N)
Z'	Non-dimensional heave force, $Z/(0.5\rho U_0^2 L_{OA}^2)$

β	Drift angle ($^\circ$)
ρ	Fluid density ($kg m^{-3}$)
μ	Fluid dynamic viscosity ($kg m^{-1} s^{-1}$)
ν	Fluid kinematic viscosity ($m^2 s^{-1}$)
∇	Volume displacement (m^3)

Introduction

When a submarine executes a turn in the horizontal plane, observations have pointed out that it tends to pitch bow up/stern down during the turn [5]. This phenomenon is known as "stern dipping" and has implications for stability, control, stealth, and safe operation of submarines, especially for manoeuvres in littoral waters or near the free surface.

Stern dipping is generally recognised as occurring due to the effects of the sail tip vortex over the stern of the submarine (see figure 1) [4, 5, 6]. The sail vortex opposes the hull circulation and induces a higher pressure field on the deck region compared to the keel region at the stern of the submarine, as shown in figure 2. This pressure difference results in a downward force on the stern of the submarine and is considered an out-of-plane load as it is out of the manoeuvring plane.

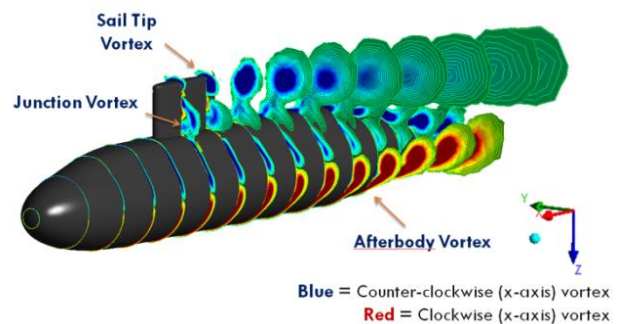


Figure 1. Axial vortices shedding from the submarine geometry turning to port in the horizontal plane (leeward side). The submarine geometry is without control planes and propulsor.

The mechanism of the sail tip vortex leading to the stern dipping phenomenon for a submarine turning has been well established experimentally [1, 4] and numerically [6]. The studies highlight the effects of the sail tip vortex by quantify the total pitching moment and heave force acting on a submarine moving either at a drift angle or undergoing a steady turn. This paper complements the above studies by numerically examining the resulting downward force distribution over a submarine undergoing a steady turn due to the sail tip vortex. In addition, the casing contributions to the downward force are also presented.

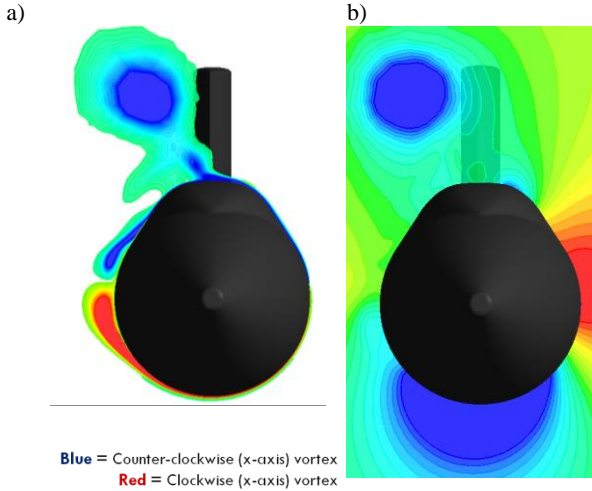


Figure 2. Flow structures at a vertical normal cutplane located at midpoint between the sail tip and stern tip (looking from the stern) of the submarine turning to port in the horizontal plane. **a)** Velocity curls outlining the vortices shedding from the submarine. **b)** Pressure distribution around the submarine following a rainbow contour scheme with red and blue indicating high and low pressures respectively.

Investigation Programme

The submarine shape used in this study is based on the Defence Science and Technology (DST) Group developed generic Joubert submarine geometry which represents a contemporary conventional submarine [2]. Figure 3 illustrates the turning manoeuvre adopted in this study, where the submarine undergoes a steady turn to port. The turning manoeuvre was chosen to coincide with the captive-model tests on the widely studied SUBOFF submarine by Toxopeus et al. [7] for the validation of the CFD approach adopted in this study. Readers are referred to Leong et al. [3] for the validation study. The non-dimensional rotational velocity, r' is defined as:

$$r' = \frac{r \cdot L_{OA}}{U_0} = \frac{L_{OA}}{R}$$

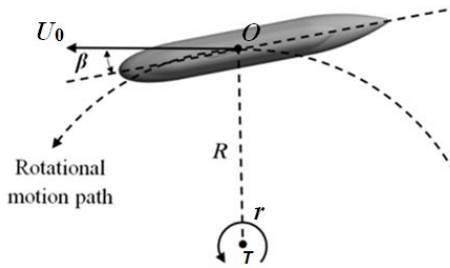


Figure 3. Description of the steady turn manoeuvre where U_0 is the linear velocity at centre of the vehicle's local coordinate system, O is the centre of the body fixed coordinate system, R is the turning radius, T is the turning point, and r is the rotational velocity.

The body fixed coordinate system used as the reference for the moment calculations and turning radius is located longitudinally at the vessel's centre of buoyancy and vertically in-line with the vessel's nose tip (see figure 4). The coordinate system follows the right hand rule with the z -direction pointing downwards. The simulations of the turning manoeuvre were conducted with a turning radius ratio (R/L) of 2.685 and a drift angle of 18 degrees (a deliberately high angle in order to exaggerate the hydrodynamic contribution of the casing and sail).

In order to isolate the downward force contributions of the sail and casing during the steady turn manoeuvre, three

configurations were examined: bare hull; hull and casing; and finally hull, casing and sail (see figure 5). None of these configurations were appended with sailplanes, aft control planes or propeller, as the study focused on the out-of-plane force generated during a turn due to the hydrodynamic effects of the casing and sail.

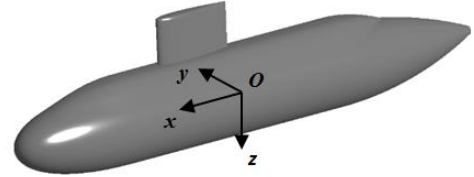


Figure 4. Body fixed coordinate system with the origin (O) located horizontally at the submarine's centre of buoyancy and vertically in-line with its nose tip.

Bare hull (BH)



Hull + Casing (HC)



Hull + Casing+ Sail (HCS)



Figure 5. Joubert submarine model configurations (from top to bottom): bare hull; hull and casing; and hull, casing and sail.

	Configurations		
	Bare hull	With Casing	With Casing and Sail
Length overall, L_{OA}	70m		
Breadth, B	9.6m		
Vertical location of the centre of origin (from keel), VC	4.8m		
Longitudinal location of the centre of origin (from nose tip), LC	37.42m	32.35m	32.31m
Volume displacement, ∇	3981m ³	4230m ³	4307m ³
Drift angle, β	18°		
Turning radius ratio, R/L	2.685		
Rotational velocity, r	2.192° s ⁻¹		
Linear velocity of the rotation at the vehicle's centre of origin, U_0	7.2m s ⁻¹		
Fluid Density, ρ	9.983 × 10 ² kg m ⁻³		
Fluid dynamic viscosity, μ	1.028 × 10 ⁻³ kg m ⁻¹ s ⁻¹		

Table 1. Geometric parameters of the submarine configurations and test conditions.

The CFD simulations in this work uses the full scale Joubert geometry thus eliminating any scaling effects. The overall length (L_{OA}) of the submarine was used as the characteristic length for

the non-dimensionalisation of the hydrodynamic forces and moments. A summary of the principal dimensions for the three configurations and the test conditions is given in table 1.

CFD Simulation Setup

The commercial CFD code, ANSYS-CFX 16, was used to model the flow around the different configurations of the submarine undergoing the steady turn manoeuvre using Reynolds-Averaged Navier Stokes (RANS) based steady state simulations. The simulation fluid domain setup and boundary conditions from Leong et al. [3] are adopted in this study for the steady turn manoeuvre as it has shown to be accurate to reproduce force and moment measurements from rotating arm experiments.

Figure 6 shows the computational domain and coordinate systems for the simulation of the turning manoeuvre. A semicircle domain was used instead of a full circle in order to prevent the submarine from interacting with its own wake. The body fixed coordinate system is shown with its origin located at the longitudinal centre of buoyancy and the global coordinate system located at centre of the semicircle domain. To simulate the submarine undergoing the steady turn, the body was moved in a rotating frame along with the domain at the rotational velocity as outlined in table 1. The submarine hull was defined as a no-slip wall; the top, inner-ring, outer-ring and bottom boundaries defined as free-slip walls to ensure that no boundary layer developed at the domain boundaries; the outlet defined as an opening with zero relative pressure; and the inlet defined as an inlet with a cylindrical flow velocity based on the rotational velocity of the domain.

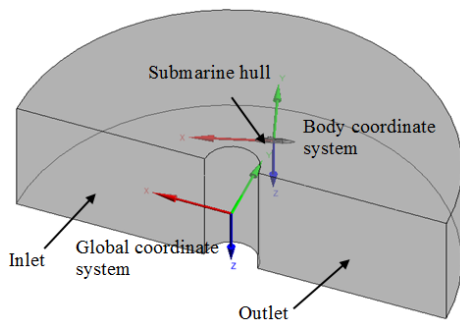


Figure 6: Computational domain and coordinate systems for the submarine steady turn manoeuvre.

The computational mesh was generated with the ANSYS Meshing Platform and is composed of triangular prismatic layers around the body to capture the boundary layer and unstructured tetrahedrons in the far field (see figure 8). A y^+ of 1 is used for the first prismatic layer height in combination with the Baseline Reynolds Stress turbulence model as it provides a consistent accuracy for force and moment predictions of axis-symmetrical bodies undergoing a steady turn with different drift angles, as investigated by the authors in the inflation layer studies described in [3]. The overall cell count for the hull, casing and hull configuration used in this study was 8 million which was deemed sufficient for the purpose of this study as it provided deviations in forces and moments below 2% when compared to subsequent mesh refinements of up to 16 million, with the Z' and M' results shown in figure 7.

The ANSYS “high resolution” advection scheme was used for the simulations. The convergence criteria for the solver results were force and moment fluctuations of no more than 3 significant figures over 100 iterations, global residual root mean square values of less than 1×10^{-4} , and global imbalances of less than 1%.

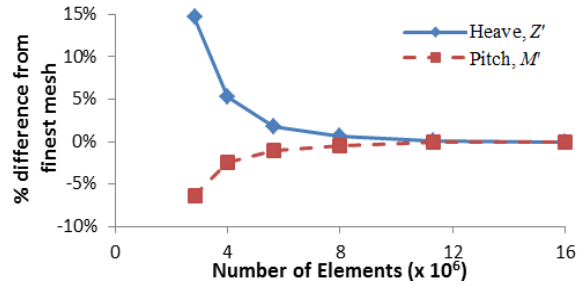


Figure 7: Percentage difference of the non-dimensional heave force Z' and pitching moment M' , predictions from the finest 16 million mesh.

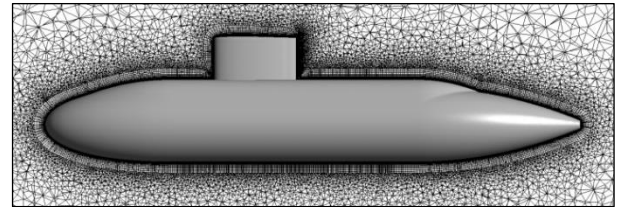


Figure 8. Mesh model of the Joubert hull, casing and sail (HCS) configuration.

Results and Discussion

Figure 9 shows the total out-of-plane loads, i.e. heave force and pitching moment, on the three configurations undergoing the steady turn manoeuvre. A positive value for Z' and M' indicates a downward force and stern-down moment respectively.

For the bare hull, the resulting heave force and pitching moment were zero, and thus the body will maintain even trim and depth when turning. The addition of the casing generates an upward force and slight stern-up moment. The largest out-of-plane load is attributed to the addition of sail which results in a substantial downward force and stern-down moment.

Figure 10 shows the downward force distribution along the longitudinal axis of the three configurations undergoing the steady turn. The casing is shown to induce an overall upward force distribution. The combination of the casing and sail are shown to induce a substantial overall downward force distribution, especially aft of the sail tip.

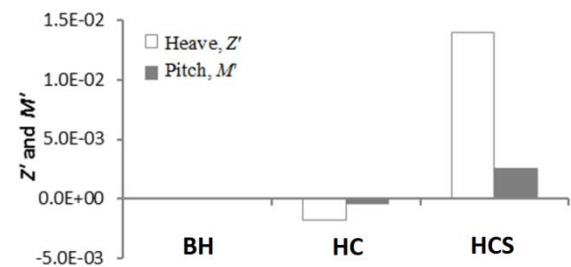


Figure 9. Non-dimensional heave force Z' and pitching moment M' for the three configurations undergoing the steady turn manoeuvre: bare hull (BH); hull and casing (HC); and hull, casing and sail (HCS).

The observations can be attributed to the effects of the casing and sail on the flow structure around the submarine. These effects are visualised in Figure 11, which shows the development of the axial vortices for the three configurations undergoing the steady turn manoeuvre. For the bare hull, the top and bottom counter-rotating vortices are symmetrical in the horizontal plane, hence the heave force and pitching moment are zero. The addition of the casing reduces the size of the upper downstream vortices

especially towards aft end of the casing. This produces a circulation around the hull that gives rise to a slightly larger pressure below the hull in that region, in turn resulting in an upwards force. With the addition of the sail, a strong counter-clockwise vortex develops downstream from the sail tip, which is much larger than the bottom clockwise vortex. This results in a much stronger circulation in the opposite sense giving a pronounced downward force distribution acting on the stern of the submarine. In comparison to the casing only configuration, the vertical force is greater in magnitude and spans the length of the hull aft of the fin. This is due to the much stronger tip vortex affecting the flow structure around the hull.

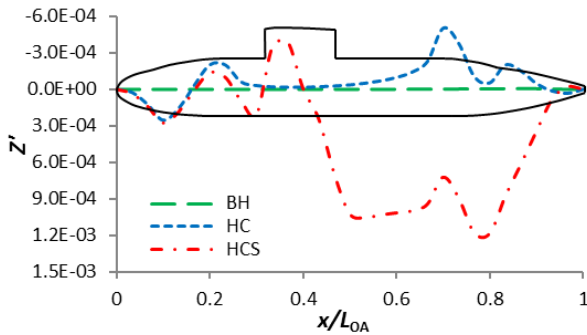
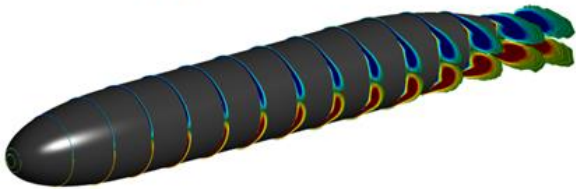


Figure 10. Non-dimensional heave force Z' distribution along the longitudinal axis of the three Joubert configurations undergoing the steady turn manoeuvre: bare hull (BH); hull and casing (HC); and hull, casing and sail (HCS).

Bare hull (BH)



Hull + Casing (HC)



Hull + Casing+ Sail (HCS)

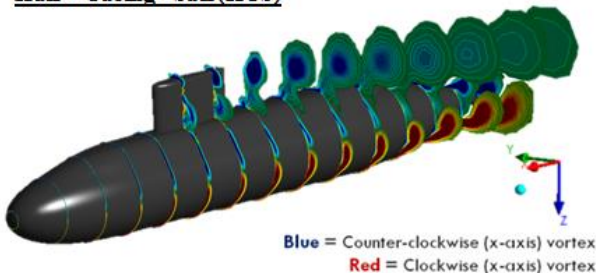


Figure 11. Axial vortices shedding from the three Joubert configurations undergoing the steady turn manoeuvre (from top to bottom): bare hull (BH); hull and casing (HC); and hull, casing and sail (HCS).

Concluding comments

This study numerically examined the out-of-plane loads which pitch down the stern of a submarine (stern dipping) undergoing a

turning manoeuvre in the horizontal plane at a high drift angle. Three different submarine configurations: bare hull; hull and casing; and hull, casing and sail, were investigated in order to isolate the out-of-plane load contributions of the submarine casing and sail to the stern dipping behaviour.

The downstream vortex of the sail tip is shown to generate a flow structure around the submarine hull that results in a large downward force distribution on the stern of the submarine. Flow visualisation of the axial vortices shedding from the submarine was used to illustrate the causative effects of the sail and casing on the flow recirculation around the submarine which results in the out-of-plane loads. Depending on the relative size of the vortices between the upper and lower regions of the submarine, the out-of-plane load will act towards the direction of the region with smaller vortices.

The vortices of the bare hull configuration were symmetrical in the horizontal plane, and thus no out-of-plane loads were observed. The addition of the casing and sail acts to respectively reduce and increase the size of the vortices in the upper half of the submarine. However, the vortex shed from the sail tip is substantially larger than vortex contributions from the casing and lower region of the hull, resulting in the pronounced downward force distribution along the stern of the submarine. This is shown to be the main cause of the stern dipping phenomenon.

Further work is being undertaken to quantify the recirculation effects of the sail, casing and hull of a submarine undergoing a steady turn and the 'stern dipping' dependence on the submarine turning angle, turning rate, and the shape and location of the submarine hull and sail. The results generated are intended to be used in dynamic submarine manoeuvring simulations and to contribute towards improved hydrodynamic design and operation of submarines.

References

- [1] David, H.B., *A Detailed Study of the Flow Field of a Submarine at Large Angle of Drift*, Mississippi State University, 2001.
- [2] Joubert, P., *Some Aspect of Submarine Design – Part 2. Shape of a Submarine 2026*, DSTO Technical Report, DSTO-TR-1920, 2006.
- [3] Leong, Z.Q., Ranmuthugala, D., Penesis, I. & Nguyen, H.D., RANS-based CFD Prediction of the Hydrodynamic Coefficients of DARPA SUBOFF Geometry in Straight-Line and Rotating Arm Manoeuvres, *RINA International Journal of Maritime Engineering*, 157, 41-51, 2015.
- [4] Mackay, M., *A Review of Submarine Out-of-Plane Normal Force and Pitching Moment*, Defense R&D Canada-Atlantic, 2004.
- [5] Renilson, M., *Submarine Hydrodynamics*, London, Springer, 2015, ISSN: 2191-530X, ISBN: 978-3-319-16183-9.
- [6] Seil, G.J. & Anderson, B., A Comparison of Submarine Fin Geometry on the Performance of a Generic Submarine, in *Proceedings of Pacific 2012 International Maritime Conference, Sydney, 2012*.
- [7] Toxopeus, S. L., P. Atsavapranee and W. Eric (2012). Collaborative CFD exercise for a submarine in a steady turn. Proceedings of ASME 31st International Conference on Ocean, Offshore and Arctic Engineering, Rio de Janeiro, Brazil.